HHS Public Access

Author manuscript

J Am Chem Soc. Author manuscript; available in PMC 2019 January 04.

Published in final edited form as:

J Am Chem Soc. 2015 April 29; 137(16): 5569–5575. doi:10.1021/jacs.5b02156.

Structural Elucidation and Synthesis of Eudistidine A: An Unusual Polycyclic Marine Alkaloid that Blocks Interaction of the Protein Binding Domains of p300 and HIF-1α

Susanna T. S. Chan[†], **Paresma R. Patel**[‡,§], **Tanya R. Ransom**[†], **Curtis J. Henrich**[†,⊥], **Tawnya C. McKee**[†,#], **Andrew K. L. Goey**[‖], **Kristina M. Cook**[‖], **William D. Figg**[‖], **James B. McMahon**[†], **Martin J. Schnermann**[*,‡], and **Kirk R. Gustafson**[*,†]

[†]Molecular Targets Laboratory, Center for Cancer Research, National Cancer Institute, Frederick, Maryland 21702-1201, United States

[‡]Chemical Biology Laboratory, Center for Cancer Research, National Cancer Institute, Frederick, Maryland 21702-1201, United States

[§]National Center for Advancing Translational Sciences, National Institutes of Health, Bethesda, Maryland 20892, United States

[⊥]Basic Science Program, Leidos Biomedical Research, Inc., Frederick National Laboratory for Cancer Research, Frederick, Maryland 21702-1201, United States

[‖]Genitourinary Malignancies Branch, Center for Cancer Research, National Cancer Institute, Bethesda, Maryland 20892, United States

Abstract

Low oxygen environments are a hallmark of solid tumors, and transcription of many hypoxia-responsive genes needed for survival under these conditions is regulated by the transcription factor HIF-1 (hypoxia-inducible factor 1). Activation of HIF-1 requires binding of its α-subunit (HIF-1α) to the transcriptional coactivator protein p300. Inhibition of the p300/HIF-1α interaction can suppress HIF-1 activity. A screen for inhibitors of the protein binding domains of p300 (CH1) and HIF-1α (C-TAD) identified an extract of the marine ascidian *Eudistoma* sp. as active. Novel heterocyclic alkaloids eudistidines A (**1**) and B (**2**) were isolated from the extract, and their structures assigned by spectroscopic analyses. They contain an unprecedented tetracyclic core composed of two pyrimidine rings fused with an imidazole ring. Eudistidine A (**1**) was synthesized in a concise four-step sequence featuring a condensation/cyclization reaction cascade between 4-(2-aminophenyl)pyrimidin-2-amine (**3**) and 4-methoxy-phenylglyoxal (**4**), while eudistidine B (**2**) was synthesized in a similar fashion with glyoxylic acid (**5**) in place of **4**.

[*]**Corresponding Authors:** gustafki@mail.nih.gov, martin.schnermann@nih.gov.

[#]**Present Address:** T.C.M.: Diagnostic Biomarkers and Technology Branch, Cancer Diagnosis Program, DCTD, National Cancer Institute, Bethesda, Maryland 20850, United States.

Supporting Information

General experimental, isolation, synthesis, ^{1}H NMR, ^{13}C NMR, COSY, HSQC, HMBC, and ROESY, together with HRESIMS and UV–vis data for compounds **1** and **2**. p300/HIF-1α testing data for compound **1**. This material is available free of charge via the Internet at http://pubs.acs.org.

The authors declare no competing financial interest.

Naturally occurring eudistidine A (**1**) effectively inhibited CH1/C-TAD binding with an IC_{50} of 75 μM, and synthetic **1** had similar activity. The eudistidine A (**1**) scaffold, which can be synthesized in a concise, scalable manner, may provide potential therapeutic lead compounds or molecular probes to study p300/HIF-1α interactions and the role these proteins play in tumor response to low oxygen conditions. The unique structural scaffolds and functional group arrays often found in natural products make these secondary metabolites a rich source of new compounds that can disrupt critical protein−protein binding events.

Graphical Abstract

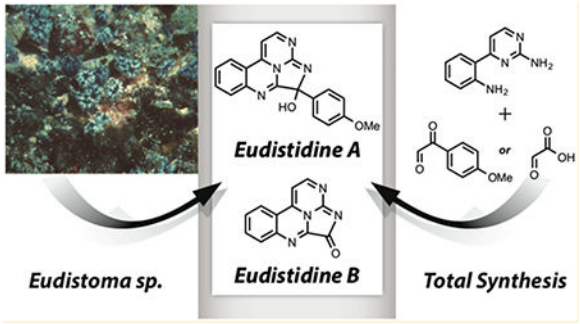

INTRODUCTION

Hypoxia is a condition characteristic of many solid tumors that results from accelerated cellular proliferation and inadequate vascularization. The transcription factor HIF-1 (hypoxiainducible factor 1) is critical for initiating adaptive responses to low oxygen environments and maintaining cellular homeostasis. HIF-1 regulates the transcription of numerous hypoxia-responsive genes, including ones that modulate glycolysis and glucose flux, and those associated with vasodilation and angiogenesis such as vascular endothelial growth factor.[1,2] Overexpression or dysregulation of HIF-1 function has been implicated in tumor progression, metastasis, resistance to chemotherapies, and poor clinical outcomes for a variety of tumor types.[3,4] While inhibition of HIF-1 function has long been recognized as an attractive potential anticancer target,[5] effective chemotherapeutic agents that can modulate or target HIF-1 activity are still needed.[6]

HIF-1 is a heterodimer of α- and β-subunits, and the transcriptional activity of this complex is regulated by either the accumulation or turnover of the HIF-1α monomer.[7] Under normoxic conditions, HIF-1α is rapidly recycled in a process that involves hydroxylation of specific proline residues, followed by ubiquitination and proteasomal degradation of the monomer.[8] When oxygen tension is low, HIF-1α accumulates in the nucleus where it dimerizes with the constitutively present HIF-1β subunit. This allows recruitment and binding of the transcriptional coactivator p300, a multidomain protein that not only plays a crucial role in HIF-1 activation but also has intrinsic histone acetyl transferase and polyubiquitin ligase activities.[9–12] The essential binding interaction between p300 and HIF-1 that facilitates hypoxia-induced transcription involves the cysteine histidine-rich domain 1 (CH1) of p300 and the C-terminal transactivation domain (C-TAD) of HIF-1α.[13–15] With the goal of identifying small molecule inhibitors of the p300/HIF-1α interaction,

we developed a high-throughput assay based on the methodologies of Kung et al.[16] to screen for compounds and natural product extracts that can disrupt CH1/C-TAD binding as a means of blocking HIF-1 activation and potentially inhibiting tumor response to hypoxic conditions.

RESULTS AND DISCUSSION

A high-throughput screening assay was developed that employed the N-terminal biotinylated HIF-1α C-TAD domain (aa 786–826) bound to streptavidin-coated 384 well plates and a GST-labeled p300 CH1 domain (aa 323–423). Binding of soluble CH1 to the immobilized C-TAD was measured by the fluorescence of a europium-tagged anti-GST antibody. The CH1/C-TAD binding interaction is very strong, as it forms a highly ordered complex with 3393 Å^2 of buried surface area.[14] The hit rate from a screen for small molecule inhibitors of this protein–protein interaction was anticipated to be very low. Prior screening of a library of 600 000 pure compounds using a similar CH1/C-TAD system provided only a single lead compound.[16] A primary focus of the current study was to mine the vast chemical diversity of the NCI's Natural Products Repository, which contains extracts from taxonomically diverse terrestrial plants, marine invertebrates, and microbial isolates.[17] Our testing of >158 000 crude natural product extracts and prefractionated extract samples for inhibition of CH1/C-TAD binding identified 27 confirmed hits. One of these was a relatively polar fraction from the organic solvent extract of the colonial marine ascidian *Eudistoma* sp. collected in Palau that exhibited significant activity; therefore, detailed chemical studies were initiated. Bioassay-guided fractionation of the crude extract employing a combination of diol SPE cartridges and repeated Sephadex LH-20 column chromatography provided two new compounds that were named eudistidine A (**1**) and eudistidine B (**2**).

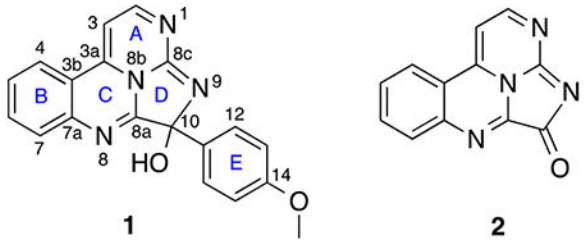

Eudistidine A (**1**) was isolated as an optically inactive green oil with a molecular formula of $C_{19}H_{14}N_4O_2$ that was established by HRESI mass spectrometry and required 15 degrees of unsaturation. The highly aromatic character of **1** was apparent from the presence of 17 sp^2 carbons and only two sp^3 carbon signals (δ_C 55.1 and 94.4) in the ^{13}C NMR spectrum (Table 1). Resonances attributable to 10 aromatic protons (δ_H 8.54, 8.40, 7.92, 7.85, 7.71, 7.54, 6.95, 6.91), one methoxyl (δ_H 3.74, 3H), and one hydroxyl group (δ_H 6.86) were observed in the ^{1}H NMR spectrum (DMSO-d_6). COSY NMR data identified the presence of three proton–proton spin-systems: a 1,2-disubstituted benzene ring [δ_H 8.40 (d, J = 8.2 Hz), 7.92 (dt, J = 1.1, 7.6 Hz), 7.85 (d, J = 8.0 Hz), 7.71 (dt, J = 1.0, 7.6 Hz)], a *para*-substituted benzene ring [(δ_H 7.54, 2H (d, J = 8.8 Hz), 6.91, 2H (d, J = 8.9 Hz)], and two mutually coupled heteroaromatic protons [(δ_H 8.54 (d, J = 4.9 Hz), 6.95 (d, J = 4.8 Hz)]. HSQC and HMBC data confirmed both the 1,2-disubstituted benzene ring (designated as ring B) and

the *para*-substituted benzene ring (ring E), and established the presence of a methoxyl group on the latter ring (Figure 1).

Deshielded carbon and proton chemical shifts (δ_C 166.2/δ_H 8.54) observed for the C-2 aromatic methine indicated it was situated directly adjacent to a nitrogen, while the highly shielded signals for C-3 (δ_C 92.2/δ_H 6.95) suggested the presence of additional nitrogen functionality in ring A. The position of C-3a in the A ring and linkage to ring B were revealed by HMBC correlations from H-2, H-3, and H-4. An HMBC correlation from H-3 to C-3b confirmed the A-B ring linkage, while the deshielded chemical shift of C-3a (δ_C 144.5) indicated it was directly bound to a nitrogen atom. An HMBC correlation from H-2 to a quaternary carbon resonance at δ_C 154.8 (C-8c) suggested this carbon was part of a conjugated guanidino moiety. This functionality could be accommodated by linking C-8c with the nitrogen (N-8b) that was also joined to C-3a, to give a pyrimidine core for ring A. Observed correlations in the HMBC spectrum from protons at δ_H 8.40 (H-4) and 7.92 (H-6) to a deshielded carbon resonance δ_C 145.7 (C-7a), and from δ_H 7.85 (H-7) and 7.71 (H-5) to δ_C 117.0 (C-3b) suggested that ring B was fused with another nitrogen-containing heterocycle (ring C). A weak 4-bond HMBC correlation from H-3 in ring A to a carbon resonance at δ_C 160.0 was also observed. The deshielded nature of this aromatic carbon suggested it was directly bound to more than one nitrogen atom, and the fact that no other HMBC correlations were observed indicated it was remote from all other aromatic protons. This carbon (C-8a) was assigned to a second fused pyrimidine ring (ring C) that incorporated nitrogens N-8 and N-8b, and was situated between rings A and B. $^{1}H–^{15}N$ HMBC correlations from H-2 and H-3 to N-1 (δ_N 255.9), H-3 to N-8b (δ_N 164.0), and H-7 to N-8 (δ_N 254.2) supported both this assignment and the fused nature of rings A, B, and C.

HMBC correlations observed from the methoxyl protons (δ_H 3.74) to a carbon resonance at δ_C 159.1 (C-14), as well as from the aromatic protons at δ_H 7.54 (H-12/H-16) to C-14 and from δ_H 6.91 (H-13/H-15) to both δ_C 133.4 (C-11) and 113.3 (C-13/C-15), defined the *para*-methoxy-substituted benzene ring (E). A correlation from the H-12/H-16 protons to a quaternary carbon resonance at δ_C 94.4 revealed this carbon (C-10) was the connection point between ring E and the rest of the molecule. The chemical shift of C-10 was appropriate for a hemiaminal functionality, and this was supported by an HMBC correlation from the hydroxyl proton at δ_H 6.86 to C-10. An HMBC correlation from the OH proton to C-8a (δ_C 160.0) also revealed that C-8a and C-10 were adjacent. One additional ring was needed to satisfy the unsaturation equivalents implicit in the molecular formula of **1**. This was accommodated by linking together C-10 and N-9 to form a fused imidazole ring (D), which then completed the planar structural assembly of eudistidine A (**1**). The pentacyclic framework of eudistidine A (**1**) contains several novel structural elements. Specifically, the 4-hydroxy, 4-aryl, 5-imino dihydroimadzole ring system and the fused pyrimido-quinazoline heterocycle are unprecedented in the natural product literature. These rare structural features are suggestive of an unusual biogenesis of **1**.

The extended π-conjugation of eudistidine A (**1**) prompted us to investigate its UV absorption properties. While only sparingly soluble in methanol, **1** showed excellent solubility in DMSO and good aqueous solubility. UV absorption maxima in DMSO were observed at 327 and 450 nm. In aqueous solutions the absorption profile was strongly pH

dependent. Local absorption maxima were observed at 393 and 440 nm in acidic and basic conditions, respectively, and an isosbestic point at 407 nm (Figure 2). The pK_a of the titratable proton in **1** was 5.1 ± 0.1 (Supporting Information).

Eudistidine A (**1**) was isolated as an optically inactive compound (no optical rotation $[\alpha]_D$ or Cotton effects in the CD spectrum when recorded in DMSO); thus, the natural product is racemic. While a ring-opened tautomeric structure of **1** can be envisioned (Figure 3), the presence of both a sharp hydroxyl proton signal (δ_H 6.86) and a hemiaminal carbon resonance (δ_C 94.4), and the lack of any signal for a ketone carbon in either the ^{13}C NMR spectrum or the IR spectrum of **1**, indicated that the cyclized form is predominant under all conditions examined to date.

Eudistidine B (**2**) was isolated as a yellow-green oil, and its molecular formula of $C_{12}H_6N_4O$ was established by (+)-HRESI mass spectrometry. The molecular formula was indicative of an aromatic heterocyclic structure that incorporated 12 unsaturation equivalents. Eudistidine B (**2**) had rather poor solubility in MeOH so DMSO was used for the UV studies, which showed λ_{max} at 327 and 445 nm. Direct comparison of the NMR data for **2** (Table 2) with those obtained for eudistidine A (**1**) revealed that the hydroxyl moiety and the *para*-substituted benzene ring in **1** were not present in **2**. However, analysis of the ^1H, ^{13}C, COSY, HSQC, and HMBC NMR data confirmed that the same fused ring system substructure observed in compound **1** (rings A, B, and C) was also present in **2**. There was a consistent downfield shift for all of the protons present in eudistidine B (**2**), while the carbon resonances for C-3, C-8c, and C-10 were shifted downfield relative to those in **1**, and C-8a was shifted upfield. The most significant change was the absence of the C-10 hemiaminal carbon resonance at δ_C 94.4 and the appearance of a resonance at δ_C 172.0. This revealed the presence of an amide carbonyl functionality that was bound to nitrogen N-9, and it allowed assignment of the structure of eudistidine B (**2**). In contrast to eudistidine A (**1**), compound **2** showed no pH dependence in its UV absorption profile over a pH range of 3–11 (Figure 2), with similar absorption maxima in DMSO and water (327 and 445 nm in DMSO; 317 and 420 nm in H_2O).

While the structures of eudistidines A (**1**) and B (**2**) were assigned based on a comprehensive analysis and interpretation of their NMR spectroscopic data, the proton-deficient and heteroatom-rich nature of rings A, C, and D made definitive proof of their structures difficult. Given the unprecedented constellation of rings and heteroatoms in the eudistidines, spectral comparisons with known compounds were of limited value. We reasoned a concise total synthesis of compounds **1** and **2** would serve to both confirm the assigned structures and provide sufficient quantities of these compounds to support more detailed biological and biochemical evaluations. The general retrosynthetic approach is outlined in Scheme 1. The tautomeric structure in which the D ring is opened could feasibly be a minor component of **1**, and it is a readily apparent synthetic precursor to eudistidine A. It was envisaged that this tautomer could be formed from 4-(2-aminophenyl)pyrimidin-2-amine (**3**) and 4-methoxy-phenylglyoxal (**4**) through a sequential condensation, cyclization, and oxidation reaction process.[18–22] A related sequence with **3** and glyoxylic acid (**5**) was also anticipated to provide **2**.

In brief, the synthesis of **1** was accomplished as follows. The key precursor, 4-(2-aminophenyl)pyrimidin-2-amine (**3**), was synthesized in three steps from 1-(2-nitrophenyl)ethanone as reported previously,[21] but with a slight modification at the last step. By using Pd/C to hydrogenate 4-(2-nitrophenyl)-pyrimidin-2-amine, instead of HCl and iron as described in the literature, compound **3** could readily be prepared on a multigram scale. Intermediate **3**, which provided rings A and B and all four nitrogen atoms in **1**, was used in the subsequent step without further purification after verification of the structure by LCMS and ^{1}H NMR. The aryl glyoxal reagent **4**, predominantly as its hydrate form, was generated via a Kornblum oxidation of 2-bromo-4′-methoxyacetophenone in DMSO/water and was used immediately without further purification.[22] Efficient condensation of reagents **3** and **4**, followed by oxidative conversion to eudistidine A (**1**) was ultimately accomplished through a one-pot sequence consisting of dropwise addition of in situ generated aryl glyoxal **4** to a DMSO solution of **3**, mild heating (1 h, 65 °C) presumably to promote condensation and cyclization, and then finally in situ oxidation with one equivalent of I_2 (1 h, 65 °C). Purification of the reaction product by reversed-phase C_{18} HPLC provided compound **1** in excellent yield (70%), which was identical by MS and NMR with the natural product eudistidine A. Significant optimization was required to develop the conditions used in the final key step. For example, precondensation of the aryl glyoxal **4** with intermediate **3** prior to I_2-mediated oxidation was required, as the simultaneous addition of **4** and iodine to **3** provided **1** in only trace quantities. Moreover, evaluation of a series of different oxidants [I_2, DDQ, MnO_2, Fe(III)] in the reaction sequence revealed that iodine alone provided both a high yield of **1** and the most reproducible results.

Using a similar strategy, eudistidine B (**2**) was synthesized by heating a solution of glyoxylic acid (**5**) and 4-(2-aminophenyl)-pyrimidin-2-amine (**3**) at 60 °C for 18 h in DMF to provide the desired product **2** in 38% yield. Condensation proceeded with autoxidation and it is likely that ambient O_2 is involved in this process. However, the addition of exogenous oxidants (I_2, DDQ, or MnO_2) significantly hindered the productive reaction pathway. The spectroscopic data for the synthetic material were in complete agreement (MS, ^{1}H NMR, and ^{13}C NMR) with those obtained with the natural product, eudistidine B (**2**). The syntheses of eudistidines A (**1**) and B (**2**) were both accomplished in a concise, scalable, and economic manner with quite acceptable overall yields. These efforts help to confirm the assigned structures of the natural products and they open the way for large-scale production and analogue development.

In a dose–response format of the screening assay, naturally occurring eudistidine A (**1**) effectively blocked the binding of soluble CH1 (p300) to immobilized C-TAD (HIF-1α) with an IC_{50} of approximately 75 μM, while eudistidine B (**2**) showed no inhibition at a high dose of 250 μM. Eudistidine A (**1**) was initially isolated from the ascidian extract and characterized as its free base. Alkaloids are generally more stable as salts so several different salts were prepared by treatment of **1** with HCl, TFA, or acetic acid. While the different salt forms of **1** had a measurable impact on its observed activity in the assay, TFA salts of the natural product and synthetically prepared eudistidine A (**1**) had consistent and virtually identical inhibitory activity (Supporting Information). In an effort to evaluate a broader range of potential activities of interest, compound **1** was screened against a commercial

panel of 456 protein kinase enzymes and 32 bromodomain proteins (DiscoverRx, San Diego, CA), and it had no effect against any of these targets. These results suggest that inhibition of the CH1/C-TAD interaction by **1** is not due to a nonspecific propensity to bind to proteins, but is more specific for these two binding partners. A degree of protein target selectivity is consistent with the lack of general cytotoxic effects observed for **1** when tested at the standard concentration of 40 μM in the NCI-60 cell anticancer screen.

Protein–protein interactions play fundamental roles in a wide range of aberrant biological processes associated with disease development and progression. However, these interactions have often been viewed as “undruggable” due to the large surface area and varied topography of the protein regions that interact.[23,24] Effective small molecule inhibitors of protein–protein interactions are rare and difficult to design de novo, so efforts to disrupt protein–protein binding for potential therapeutic applications have often focused on small proteins or peptide mimetics.[25,26] Many of the small molecules that can inhibit protein–protein interactions have poor specificity or potencies in the millimolar range. With its ability to block CH1/C-TAD binding at micromolar concentrations, eudistidine A (**1**) represents an intriguing new structural scaffold for developing small molecule inhibitors of p300/HIF-1α interactions.

The p300 protein is an attractive molecular target for the identification of potential therapeutic agents, and a variety of small molecule natural products have recently been reported to interact with p300 and inhibit its acetyl transferase activity. These include the prenylated benzophenone garcinol,[27] a rearranged steroidal derivative from a marine sponge, [28] and a plant flavonoid related to quercitin.[29] Naturally occurring small molecules have also been identified that can disrupt the formation or stability of the p300/HIF-1α complex. For example, the fungal metabolite chetomin, a complex epidithiodiketopiperazine dimer derived from two serine and two tryptophan residues, was the only compound out of 600 000 screened that effectively blocked p300/HIF-1α binding.[16] Studies suggest that the redox potential of chetomin and other compounds with disulfides result in Zn^{2+} loss from p300 with a resultant alteration in its global fold.[16,30] Zinc is critical for maintaining the tertiary structure of p300 in a form that can complex with HIF-1α.[14,15] A similar mechanism involving zinc abstraction from p300 has also been proposed for the p300/HIF-1α inhibitory activity of a series of quinones and indandiones.[31] Any nonselective targeting of Zn^{2+} coordinating groups could impact many different proteins and result in a wide range of undesirable off target effects that would limit the utility of these types of agents. However, recent studies show that care must be taken when making assumptions about the selectivity and mode of action for a broad class of redox active compounds. A series of dimeric epidithiodiketo-piperazines was designed and synthesized,[32] and the lead compound was shown to selectively inhibit the p300/HIF-1α interaction. In cellular assays, it downregulated the expression of hypoxia-responsive genes, and in a murine model it significantly reduced in vivo tumor growth.[33] This study served as a proof of principle that validated small molecule targeting of the p300/HIF-1 interaction to inhibit tumors. The actinobacterial metabolite novobiocin, an aminocoumarin glycoside, disrupts the p300/HIF-1α interaction by directly binding to the HIF-1α C-TAD domain.[34] None of these natural products or other

previously reported p300/HIF-1α inhibitors are structurally related to the heterocyclic eudistidine scaffold.[35–37]

CONCLUSION

The rich chemical diversity of the NCI's library of natural product extracts was assessed in a high-throughput screening assay for inhibitors of p300/HIF-1α binding. We have isolated and identified two new compounds with a novel heterocyclic scaffold from an extract of the marine ascidian *Eudistoma* sp., one of which showed activity in the screen. Prior studies of ascidians in the genus *Eudistoma* led to the discovery of a variety of compound classes including β-carbolines (eudistomins, eudistomindins),[38,39] cyclic peptides (eudistomides),[40] macrolides (iejimalide),[41] and pyrrolopyrimidines (rigidins),[42] among others. Eudistidines A (**1**) and B (**2**) are unlike any other *Eudistoma* metabolites, and they represent a new structural class of alkaloids in which two pyrimidine rings and an imidazole ring are fused to generate an unprecedented tetracyclic core. This core ring system contains embedded guanidine and amidine functionalities, and in the case of eudistidine A (**1**) an additional hemiaminal group. The novel heterocyclic architecture of eudistidine A, originally assigned from analysis of its spectroscopic data, was confirmed by a concise four-step synthesis that employed 4-(2-aminophenyl)-pyrimidin-2-amine (**3**) and 2-(4-methoxyphenyl)-2-oxoacetaldehyde (4) as key precursors. Eudistidine B (**2**) was successfully synthesized using a similar approach that used glyoxylic acid (**5**) in place of compound **4**.

Small molecule inhibitors of specific protein–protein interactions are notoriously difficult to design and synthesize. However, the structures of many natural product secondary metabolites have apparently evolved to interact with specific biopolymer targets. Natural products therefore provide a rich source of chemical diversity for discovery of agents that can modulate protein interactions. In the present case, eudistidine A (**1**) was identified as an effective inhibitor of CH1/C-TAD binding, which is the key protein–protein interaction required to form the transcriptionally active p300/HIF-1α complex. Eudistidine A (**1**) can be readily synthesized, which should facilitate the generation of a family of analogues to help define the structural requirements for activity and provide adequate material to support additional biological studies. Since the activated p300/HIF-1α complex is required for the transcription of hypoxia-responsive genes in tumors, more extensive evaluations of eudistidine A (**1**) and related compounds are warranted. They may provide agents with potential anticancer therapeutic applications or small molecule probes to further define the roles of p300 and HIF-1α in tumor adaptations to low oxygen environments.

Supplementary Material

Refer to Web version on PubMed Central for supplementary material.

ACKNOWLEDGMENTS

We gratefully acknowledge D. Newman (NCI) for organizing and documenting the collection, the Natural Products Support Group at NCI-Frederick for extraction, and S. Tarasov and M. Dyba (Biophysics Resource Core, Structural Biophysics Laboratory, CCR) and H. Bokesch (MTL) for assistance with high-resolution mass spectrometry. This research was supported in part by the Intramural Research Program of the NIH, National Cancer Institute, Center for Cancer Research. This project was also funded in part with Federal funds from the National Cancer Institute,

National Institutes of Health, under contract HHSN261200800001E. The content of this publication does not necessarily reflect the views or policies of the Department of Health and Human Services, nor does mention of trade names, commercial products, or organizations imply endorsement by the U.S. Government.

REFERENCES

(1). Semenza GL J. Clin. Invest 2013, 123, 3664–3671. [PubMed: 23999440]

(2). Yang Y; Sun M; Wang L; Jiao BJ Cell. Biochem 2013, 114, 967–974.

(3). Tsai Y-P; Wu K-JJ Biomed. Sci 2012, 19, 102–108.

(4). Harris AL Nat. Rev. Cancer 2002, 2, 38–47. [PubMed: 11902584]

(5). Semenza GL Nat. Rev. Cancer 2003, 3, 721–732. [PubMed: 13130303]

(6). Semenza GL Drug Discovery Today 2007, 12, 853–859. [PubMed: 17933687]

(7). Wang GL; Jiang BH; Rue EA; Semenza GL Proc. Natl. Acad. Sci. U. S. A 1995, 92, 5510–5514. [PubMed: 7539918]

(8). Huang LE; Gu J; Schau M; Bunn HF Proc. Natl. Acad. Sci. U. S. A 1998, 95, 7987–7992. [PubMed: 9653127]

(9). Chen J; Li Q Epigenetics 2011, 6, 957–961. [PubMed: 21730760]

(10). Bowers EM; Yan G; Mukherjee C; Orry A; Wang L; Holbert MA; Crump NT; Hazzalin CA; Liszczak G; Yuan H; Larocca C; Saldanha SA; Abagyan R; Sun Y; Meyers DJ; Marmorstein R; Mahadevan LC; Alani RM; Cole PA Chem. Biol 2010, 17, 471–482. [PubMed: 20534345]

(11). Grossman SR; Deato ME; Brignone C; Chan HM; Kung AL; Tagami H; Nakatani Y; Livingston DM Science 2003, 300, 342–344. [PubMed: 12690203]

(12). Shi D; Pop MS; Kulikov R; Love IM; Kung AL; Grossman SR Proc. Natl. Acad. Sci. U. S. A 2009, 106, 16275–16280. [PubMed: 19805293]

(13). Gu J; Milligan J; Huang LE J. Biol. Chem 2001, 276, 3550–3554. [PubMed: 11063749]

(14). Freedman SJ; Sun Z-YJ; Poy F; Kung AL; Livingston DM; Wagner G; Eck MT Proc. Natl. Acad. Sci. U. S. A 2002, 99, 5367–5372. [PubMed: 11959990]

(15). Dial R; Sun Z-YJ; Freedman SJ Biochemistry 2003, 42, 9937–9945. [PubMed: 12924942]

(16). Kung AL; Zabludoff SD; France DS; Freedman SJ; Tanner EA; Vieira A; Cornell-Kennon S; Lee J; Wang B; Wang J; Memmert K; Naegeli H-U; Petersen F; Eck MJ; Bair KW; Wood AW; Livingston DM Cancer Cell 2004, 6, 33–43. [PubMed: 15261140]

(17). McCloud TG Molecules 2010, 15, 4526–4563. [PubMed: 20657375]

(18). Gao Q; Wu X; Jia F; Liu M; Zhu Y; Cai Q; Wu AJ Org. Chem 2013, 78, 2792–2797.

(19). Liu S; Chen R; Chen H; Deng G-J Tetrahedron Lett. 2013, 54, 3838–3841.

(20). Zhu Y-P; Fei Z; Liu M-C; Jia F-C; Wu A-X Org. Lett 2013, 15, 378–381. [PubMed: 23273132]

(21). Agarwal PK; Sharma SK; Sawant D; Kundu B Tetrahedron 2009, 65, 1153–1161.

(22). Watanabe K; Uehara F; Hiki S; Yokoshima S; Usui Y; Okuyama M; Shoda A; Aritomo K; Kohara T; Fukunaga K Preparation of 2,3,6-trisubstituted-4-pyrimidones as tau protein kinase 1 inhibitors. PCT Int. Appl, 2004085408, 07 10 2004.

(23). Wells JA; McClendon CL Nature 2007, 450, 1001–1009. [PubMed: 18075579]

(24). Surade S; Blundell TL Chem. Biol 2012, 19, 42–50. [PubMed: 22284353]

(25). Bullock BN; Jochim AL; Arora PS J. Am. Chem. Soc 2011, 133, 14220–14223. [PubMed: 21846146]

(26). Azzarito V; Long K; Murphy NS; Wilson AJ Nat. Chem 2013, 5, 161–173. [PubMed: 23422557]

(27). Balasubramanyam K; Altaf M; Varier RA; Swaminathan V; Ravindran A; Sadhale PP; Kundu TK J. Biol. Chem 2004, 279, 33716–33726. [PubMed: 15155757]

(28). Gong J; Sun P; Jiang N; Riccio R; Lauro G; Bifulco G; Li T-J; Gerwick WH; Zhang W Org. Lett 2014, 16, 2224–2227. [PubMed: 24694058]

(29). Holzhauser S; Freiwald A; Weise C; Multhaup G; Han C-T; Sauer S Angew. Chem., Int. Ed 2013, 52, 5171–5174.

(30). Cook KM; Hilton ST; Mecinović J; Motherwell WB; Figg WD; Schofield CJ J. Biol. Chem 2009, 284, 26831–26838. [PubMed: 19589782]

(31). Jayatunga MKP; Thompson S; McKee TC; Chan MC; Reece KM; Hardy AP; Sekirnik R; Seden PT; Cook KM; McMahon JB; Figg WD; Schofield CJ; Hamilton AD Eur. J. Med. Chem 2015, 94, 509–516. [PubMed: 25023609]

(32). Block KM; Wang H; Szabó LZ; Polaske NW; Henchey LK; Dubey R; Kushal S; László CF; Makhoul J; Song Z; Meuillet EJ; Olenyuk BZ J. Am. Chem. Soc 2009, 131, 18078–18088. [PubMed: 20000859]

(33). Dubey R; Levin MD; Szabo LZ; Laszlo CF; Kushal S; Singh JB; Oh P; Schnitzer JE; Olenyuk BZ J. Am. Chem. Soc 2013, 135, 4537–4549. [PubMed: 23448368]

(34). Wu D; Zhang R; Zhao R; Chen G; Cai Y; Jin J PLoS One 2013, 8, e62014. [PubMed: 23671581]

(35). Kwon HS; Kim D-R; Yang EG; Park YK; Ahn H-C; Min S-J; Ahn D-R Bioorg. Med. Chem. Lett 2012, 22, 5249–5252. [PubMed: 22789427]

(36). Yang H; Pinello CE; Luo J; Li D; Wang Y; Zhao LY; Jahn SC; Saldanha SA; Planck J; Geary KR; Ma H; Law BK; Roush WR; Hodder P; Liao D Mol. Cancer Ther. 2013, 12, 610–620. [PubMed: 23625935]

(37). Na Y-R; Han K-C; Park H; Yang EG Biochem. Biophys. Res. Commun 2013, 434, 879–884. [PubMed: 23618863]

(38). Rinehart KL, Jr.; Kobayashi J; Harbour GC; Gilmore J; Mascal M; Holt TG; Shield LS; Lafargue FJ Am. Chem. Soc 1987, 109, 3378–3387.

(39). Kobayashi J; Cheng J-F; Ohta T; Nozoe S; Ohizumi Y; Sasaki TJ Org. Chem 1990, 55, 3666–3670.

(40). Whitson EL; Ratnayake AS; Bugni TS; Harper MK; Ireland CM J. Org. Chem 2009, 74, 1156–1162. [PubMed: 19053188]

(41). Kobayashi J; Cheng J-F; Ohta T; Nakamura H; Nozoe S; Hirata Y; Ohizumi Y; Sasaki TJ Org. Chem 1988, 53, 6147–6150.

(42). Kobayashi J; Cheng J-F; Kikuchi Y; Ishibashi M; Yamamura S; Ohizumi Y; Ohta T; Nozoe S Tetrahedron Lett. 1990, 31, 4617–4620.

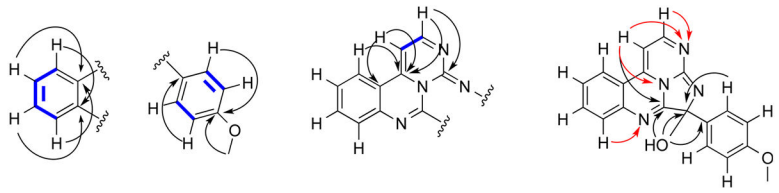

Figure 1.
Selected $^{1}H–^{13}C$ HMBC (black arrows), $^{1}H–^{15}N$ HMBC (red arrows), and COSY (bold blue lines) correlations for eudistidine A (**1**).

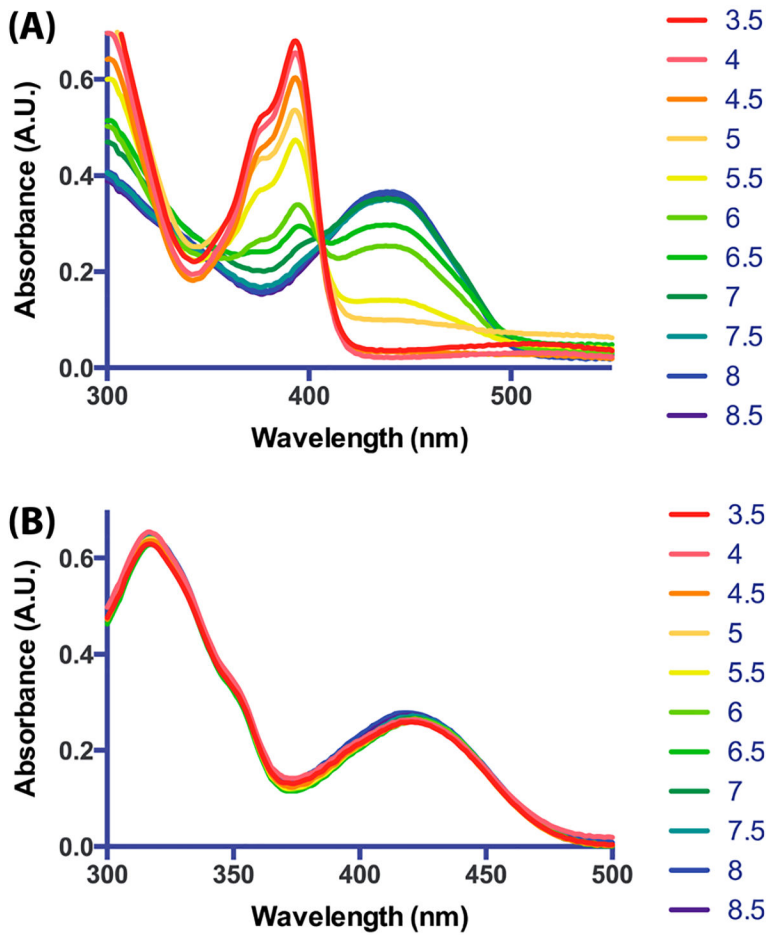

Figure 2.

pH effects on the UV absorption spectra of compound **1** (A) and **2** (B).

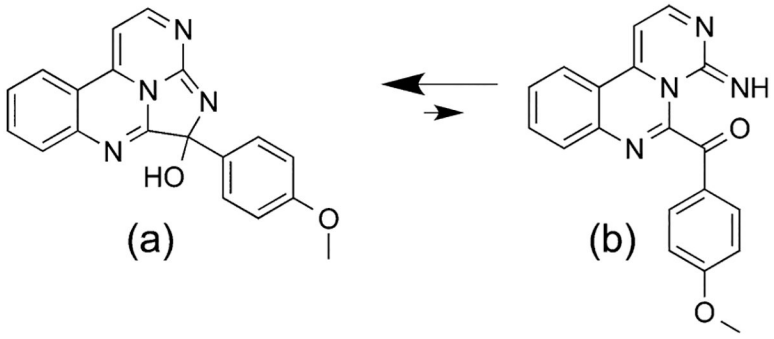

Figure 3.
Cyclized (a) and ring-opened (b) tautomers of eudistidine A.

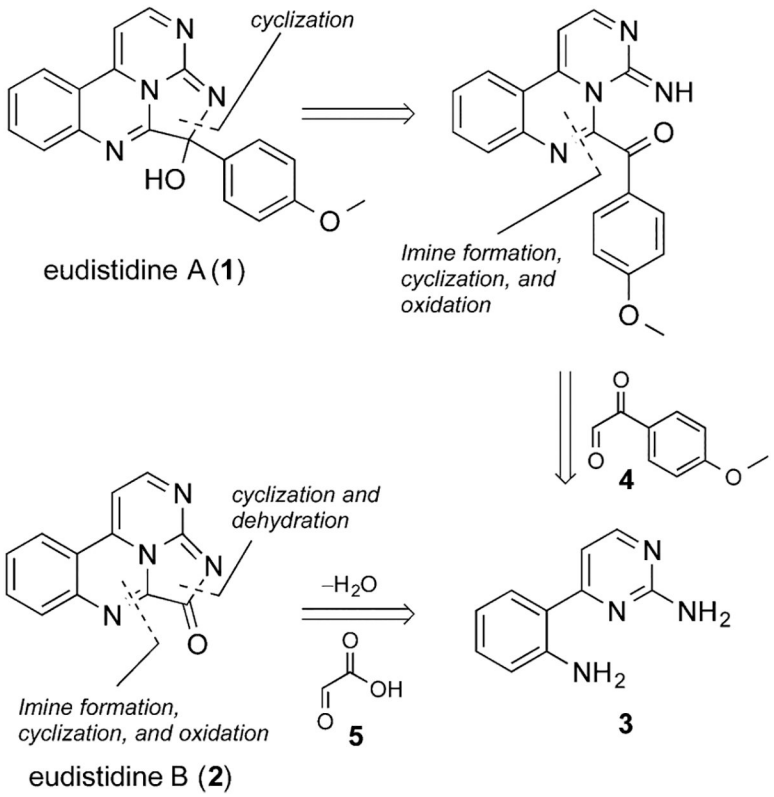

Scheme 1.
Retrosynthetic Analysis of Eudistidine A (1) and B (2)

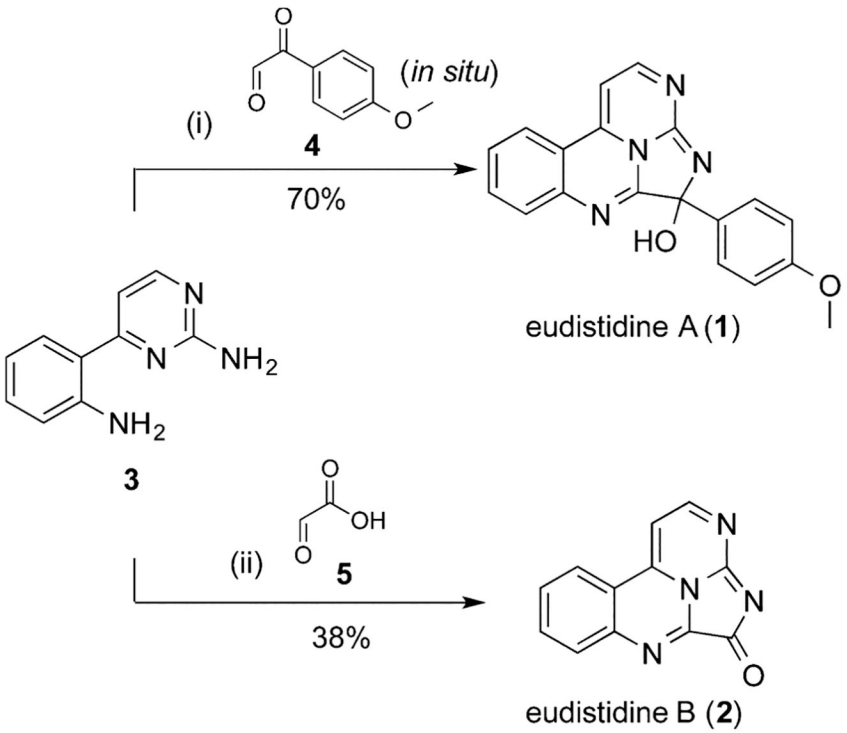

[a]Reagents and conditions: (i) DMSO, H_2O, 65 °C, 3 h; I_2, 60 °C, 1 h; (ii) DMF, 60 °C, 18 h.

Scheme 2.
Synthesis of Eudistidines A (1) and B (2)[a]

Table 1.

NMR Spectroscopic Data for Eudistidine A (1) in DMSO-d_6

position	δ_C	δ_N [a]	δ_H (mult, J in Hz)	HMBC
1		255.9		
2	166.2		8.54 (d, 4.9)	3, 3a, 3b, 8c
3	92.2		6.95 (d, 4.8)	2, 3a, 3b, 8a [c]
3a	144.5		-	-
3b	117.0		-	-
4	125.5		8.40 (d, 8.2)	3a, 6, 7a
5	128.7		7.71 (dt, 1.0, 7.6)	3b, 7
6	135.0		7.92 (dt, 1.1, 7.6)	4, 7a
7	128.6		7.85 (d, 8.0)	3b, 5
7a	145.7		-	-
8		254.2		
8a	160.0		-	-
8b		164.0		
8c	154.8		-	-
9		n.o. [b]		
10	94.4		-	-
10-OH	-		6.86 (s)	8a, 10, 11
11	133.4		-	-
12/16	127.5		7.54 (d, 8.8)	10, 11, 12/16, 14
13/15	113.3		6.91 (d, 8.9)	13/15, 14
14	159.1		-	-
14-OMe	55.1		3.74 (s)	14

[a] ^{15}N assignments were based on ^{1}H–^{15}N HMBC correlations. The δ_N values were not calibrated to an external standard but were referenced to neat NH_3 (δ 0.00) using the standard Bruker parameters.

[b] Not observed.

[c] Weak four-bond HMBC correlation.

Table 2.

NMR Spectroscopic Data for Eudistidine B (2) in DMSO-d_6

position	δ_C	δ_H (mult, *J* in Hz)	HMBC
2	163.8	9.10 (d, 5.6)	3, 3a, 8c
3	102.2	8.26 (d, 5.8)	2, 3a, 3b
3a	144.2		
3b	117.3		
4	126.5	9.00 (d, 7.9)	3a, 6, 7a
5	131.6	8.16 (t, 7.6)	3b, 7
6	136.6	8.33 (t, 7.6)	4, 7a
7	130.9	8.44 (d, 8.1)	3b, 5
7a	145.6		
8a	142.5		
8c	163.3		
10	172.0		